13th World Conference on Earthquake Engineering
Vancouver, B.C., Canada
August 1-6, 2004
Paper No. 297

PREDICTION OF DUCTILE FRACTURE IN STEEL MOMENT CONNECTIONS DURING EARTHQUAKES USING MICROMECHANICAL FRACTURE MODELS

Amit KANVINDE[1] and Gregory DEIERLEIN[2]

SUMMARY

The Northridge and Kobe earthquakes demonstrated that fracture is an important mode of failure in steel moment connections during earthquakes. Investigations conducted since these earthquakes revealed important limitations of traditional fracture mechanics in characterizing ductile crack initiation under large-scale yielding which is more likely in post-Northridge connections with smaller flaws and tougher materials. Micromechanical models that capture the fundamental mechanisms of ductile crack initiation can predict fracture even in situations of widespread yielding. This paper discusses one such model – the Stress Modified Critical Strain (SMCS) model, and its applications to realistic connection situations. The paper introduces the model and then describes a series of finite element analyses used to calibrate and apply the model to situations such as bolt-hole and Reduced Beam Section (RBS) type connection tests. It is observed that due to the relatively flat stress-strain contours in these specimens, the SMCS model can be applied using a relatively coarse mesh, indicating that the micromechanical models may be feasible for widespread use in fracture prediction. The SMCS model predicts fracture with good accuracy. The paper then describes the use of the SMCS models to transfer results between experiments, based on two different configurations of the bolt-hole experiments, where the conditions for fracture in either situation are observed to be identical when in fact the loading configuration is different. The paper concludes by referencing a larger study by the author that focused on micromechanical models for predicting low-cycle fatigue in structures during earthquakes. It is briefly noted that the micromechanical models such as the SMCS can be relatively free from assumptions and virtually extended to any loading/stress-situation because they aim to capture the fundamental mechanism of failure.

INTRODUCTION

Many experimental studies after the Northridge earthquake, such as the SAC project resulted in recommendations for developing fracture-resistant connections. These recommendations included (1) reducing the imposed toughness demands by modifying the connections – e.g. removal of backing bars or minimizing flaws through better quality control during welding (2) using notch-toughness rated materials

[1] Assistant Professor, Department of Civil and Environmental Engineering, University of California, Davis, CA 95616
[2] Professor, Department of Civil and Environmental Engineering, Stanford University, CA 94305

for base metals as well as weld metals to meet the imposed demands successfully. Other strategies such as the reduced beam connection (RBS) aimed at reducing the overall loading demand in the weld area. These studies resulted in more ductile connections, which could sustain large deformations without failing in a brittle fashion as the pre-Northridge connections.

However, studies such as Stojadinovic et al [6] showed that despite their resistance to brittle fracture, the post-Northridge type connections show ductile tearing at unacceptably low plastic hinge rotations (≈ 0.015 radians). These ductile tears accompanied by large-scale yielding have the potential to transition to cleavage type failure.

Traditional fracture mechanics, including linear elastic approaches like the K_{IC} or elastic-plastic approaches such as the J-integral or the Crack Tip Opening Displacement (CTOD) are limited by the assumption of constrained yielding, which is violated in these more ductile connections. As a result, traditional fracture mechanics approaches cannot be used reliably to predict failure under these newer situations with smaller flaws and tougher materials. Empirical, experiment-based approaches need to be relied on in order to predict performance and formulate design considerations. Empirical data of this sort cannot be directly transferred between different connection configurations and loading situations, thus raising the need for more fundamental techniques to predict ductile crack initiation. Traditional fracture mechanics indices also rely on the presence of a sharp crack or a singularity for their application. Many structural engineering components such as bolted connections, gusset plates or RBS type connections do not have sharp cracks or flaws. As a result, directly applying traditional fracture indices is somewhat of an issue in such cases.

Micromechanical models, such as the SMCS (Stress Modified Critical Strain) model applied in this paper attempt to capture the fundamental mechanism of fracture through continuum finite element analyses with failure criteria linked to the micromechanical level. In this sense, the SMCS model is to ductile fracture under multiaxial stresses and strains as the von Mises criterion is to yield under multiaxial stresses. Several earlier studies, Panontin et al [4], Hancock et al [2] have applied these models with success to non-civil engineering structures such as pressure vessels and other mechanical engineering applications. While these studies suggest that the models can be applied to evaluate fracture in buildings and bridges, work remains to validate their application for mild structural steels and to extend the models for cyclic loadings.

To address all of these issues, this study applies these micromechanical models to structural engineering situations where traditional fracture mechanics would be an inadequate tool. Two different steels – A572 Grade 50 and HPS70W are used. The SMCS model is first presented, followed by a brief overview of the calibration process using notched bar tests and finite element analyses. The calibrated model is then applied to three different experiments resembling structural connections. The SMCS model is used to make predictions of failure in these experiments, and also compare behavioral trends between the two different bolt-hole type tests. The paper concludes with a brief discussion outlining the relative convenience of applying the SMCS while summarizing some limitations.

MECHANISM FOR DUCTILE CRACK INITIATION AND THE SMCS MODEL

Mild steel, commonly used in structural engineering applications, typically exhibits ductile fracture accompanied by large scale plasticity. The stages observed during this type of fracture are observed to be those of microvoid nucleation, growth and coalescence, shown schematically in Fig. 1. Most steels contain secondary particles or inclusions such as carbides which sit in the steel matrix, around which voids nucleate under applied stresses. After nucleation, plastic strain and hydrostatic stress cause the voids to grow. Initially, the voids grow independent of one another, but upon further growth, neighboring voids

interact and eventually, plastic strain is concentrated along a certain plane of voids. At this point local necking instabilities cause the voids to grow suddenly forming the macroscopic fracture surface. In many commonly used steels, this step governs the fracture process, and the stress and strain fields governing growth and coalescence are important for predicting fracture. Fig. 2 shows a scanning electron micrograph of a surface that has fractured due to void growth and coalescence. The dimples on the surface show the locations of the voids that have coalesced.

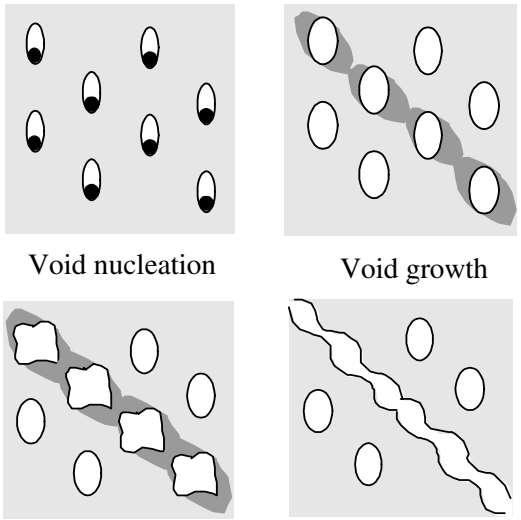

Fig. 1 – Mechanism for ductile fracture

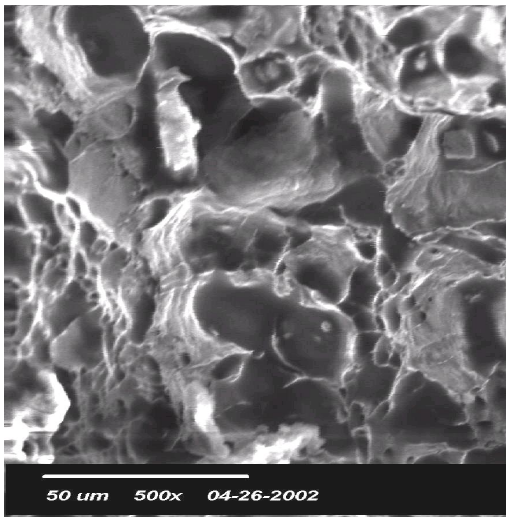

Fig. 2 – Micrograph of fractured surface showing dimples

Rice and Tracey [5] showed that the growth of a single spherical void in an elasto-plastic solid is governed by the imposed equivalent plastic strain and the triaxiality ratio as shown in equation (1).

$$\frac{dR}{R} = 0.283 \exp\left(\frac{1.5\sigma_m}{\sigma_e}\right).d\varepsilon_p \tag{1}$$

Where R is the instantaneous void radius, ε_p is the equivalent plastic strain, and the triaxiality σ_m/σ_m is a ratio of the mean stress and the effective or von Mises stress. Based on this derivation, Hancock and Mackenzie [2] proposed a simplified model – the Stress Modified Critical Strain Model (SMCS) for capturing the void growth and coalescence mechanism in metals. According to this model, ductile crack initiation occurs when the equivalent plastic strain exceeds a critical value of the plastic strain, where the critical plastic strain is a function of the triaxiality as described in equation (2).

$$\varepsilon_p > \varepsilon_p^{critical} = \alpha \cdot \exp\left(1.5\frac{\sigma_m}{\sigma_e}\right) \tag{2}$$

The constant α in equation (2) is a material parameter indicative of the material resistance to ductile crack initiation. The SMCS model captures the ductile crack initiation mechanism by taking into account the adverse effect of stress triaxiality on void growth and coalescence. A higher triaxiality will result in a lower value of critical plastic strain. The toughness index α can be calibrated based on notched round bar tests and complementary analyses as described in the next section. Another issue that is of relevance to micromechanical models is the length scale which deals with the sampling of sufficient amounts of material to cause fracture. This issue is especially important in sharp-cracked geometries that may have high stress or strain gradients at the crack tip. This paper deals with relatively blunt geometries that have

flat stress contours, and consequently the length scale issue is not of great concern, because the analytical results are largely insensitive to the choice of length scale. For more details, the reader is referred to Kanvinde [3].

CALIBRATION OF THE SMCS TOUGHNESS PARAMETER α

The SMCS parameter α is obtained through testing and finite element analyses of circumferentially smooth-notched tensile specimens – such as the one shown in Fig. 3. These test specimens have the same overall geometry as standard round tensile coupons except that they have a circumferential notch machined into them to produce a triaxial stress condition. The triaxiality is varied by changing the notch severity three different notch radii. In this study, radii of 0.06, 0.125 and 0.25 inches are employed.

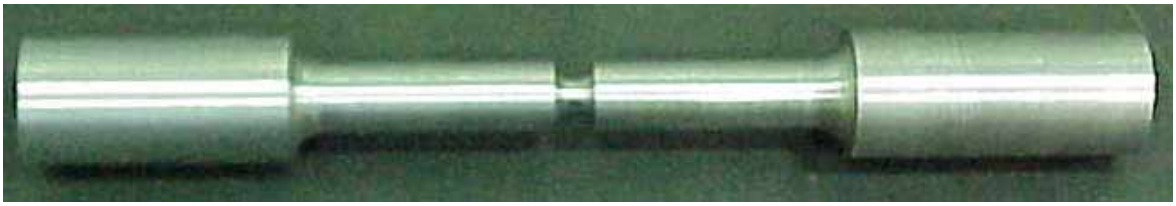

Fig. 3 – Circumferentially notched specimen for SMCS calibration

Fig. 4 shows the load versus notch elongation curve for such a test, where ductile fracture initiation is defined to coincide with sudden change in slope. One might question how closely to the point the ductile crack initiates, as opposed to fully propagate, but the flatness of the contours of the crack initiation parameters convinces us that a large crack would initiate all at once, causing the load drop.

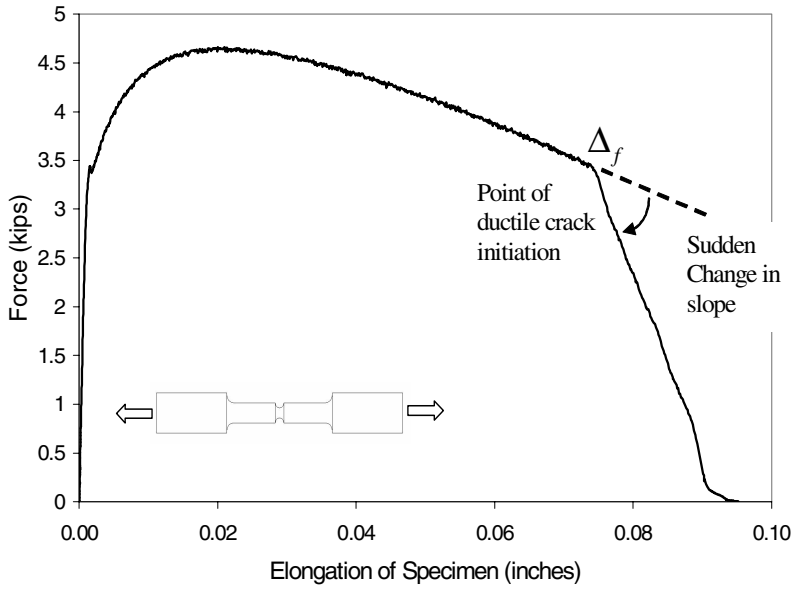

Fig. 4 – Load elongation curve for circumferentially notched calibration specimens

The critical value of the SMCS model parameter α is determined from the testing and analysis of notched tensile specimens with varying notch severity. The tests are conducted to identify the displacement corresponding to fracture initiation Δ_f shown in Fig 4. Nonlinear, elastic-plastic finite element analyses of each notched tensile geometry are performed to obtain the stresses and strains at the displacement Δ_f corresponding to fracture initiation. Substituting these critical stress and strain states at the cross section into the SMCS criterion, equation (2) to enforce a zero value at the section center determines the fracture parameter α. A sample axisymmetric finite element mesh is shown in Fig. 5.

Fig. 6 shows the triaxiality (σ_m/σ_e), plastic strain (ε_p) and SMCS $(= \varepsilon_p - \varepsilon_p^{critical})$ contours over the critical cross section of the specimen at the elongation corresponding to ductile crack initiation. Being axisymmetric, these are plotted versus distance from the bar center. A closer examination of these

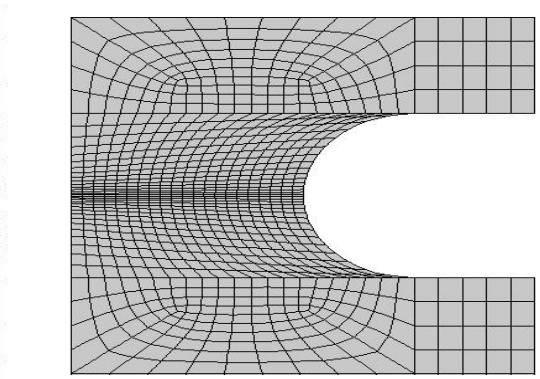

Fig. 5 – FEM Mesh

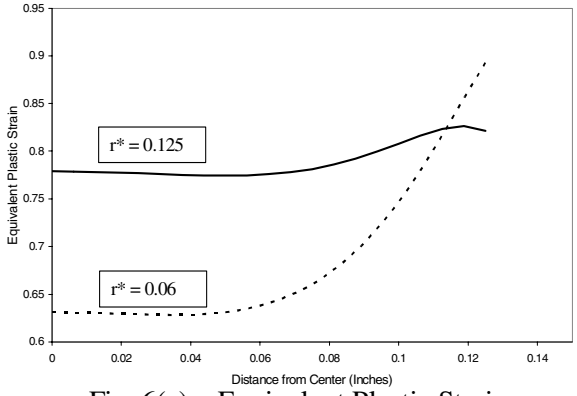

Fig. 6(a) – Equivalent Plastic Strain

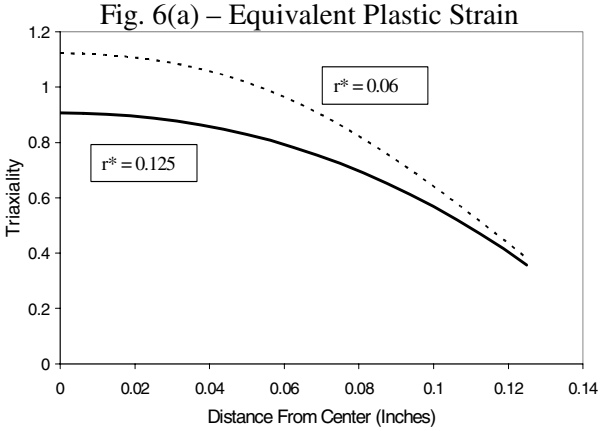

Fig. 6(b) – Triaxiality

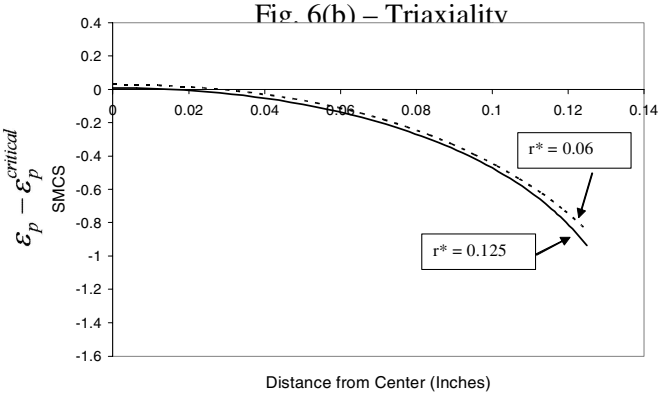

Fig. 6(c) – SMCS

quantities indicates that the triaxiality at the center of the specimens is much higher than at the free surface – Fig. 6(b) due to the higher constraint at the center However, as seen in Fig. 6(a), the equivalent plastic strain at the free surface is much higher than at the center where the fracture initiates first. The critical effective plastic strain at the center of the specimen with r* = 0.125 is much higher (by typically approximately 25%) than for r* = 0.06, whereas the triaxiality of the large-notched specimen is approximately 30% lower than the value of the smaller radius notch.

Clearly, neither of the two criteria (plastic strain or triaxiality) alone is an absolute measure of when fracture initiates. In particular, the plastic strain is not a good index, as the ductile fracture is observed to initiate at the center of the bar, as opposed to the surface, where the plastic strain is maximum. As shown in Fig. 6(c), the SMCS criterion normalizes the triaxiality and plastic strain to give a consistent fracture index for the two notched bar geometries. The SMCS plot in Fig. 6(c) reaches a critical value of zero at the center of the bar when fracture initiates in the tests. Substituting the plastic strain and triaxiality distributions into equation (2), the SMCS value is fit such that a value of zero is obtained at the center of the specimens. The α value from the different notch sizes is very similar suggesting that it can be assumed to be a material property indicative of toughness. It is very interesting to note that after combining the plastic strain and triaxiality distributions using the calculated value of α, the final SMCS distributions look identical for the different notch geometries, as can be seen from Fig. 6(c).

Table 1(a) – A572 Grade 50 Steel

Notch Size	Test #	Δ_f (inches)	α
r* =0.125"	1	0.0412	1.44
	2	0.0335	1.17
	3	0.0372	1.32
r* = 0.06"	1	0.0218	0.84
	2	0.0238	1.16
r* = 0.25"	1	0.0490	1.18
	2	0.0502	1.19
Mean			**1.18**
Coefficient of Variation			**15%**

Table 1(b) – HPS70W Steel

Notch Size	Test #	Δ_f (inches)	α
r* = 0.125"	1	0.0662	3.20
	2	0.0551	2.69
r* = 0.06"	1	0.0337	2.90
	2	0.0326	2.81
Mean			**2.90**
COV			**7%**

The low variance despite varying notch size is indicative of the capabilities of the model. The A572 Grade 50 has a much lower α value than the HPS70W, which implies that the high performance steel grade is substantially more ductile as compared to the conventional steel.

PULL-PLATE EXPERIMENTS RESEMBLING STRUCTURAL CONNECTIONS

To encourage the use of the SMCS and other micromechanical models as predictive tools, these are applied to tests with configurations similar to those commonly found in structures. This section describes a series of such tests which aim to simulate fracture using the SMCS model. These tests are run on the two steel varieties that were calibrated using the notched bar tests.

Three basic types of specimens are designed. Two of these have bolt holes and are meant to mimic members exhibiting net section failure at bolted connections. The main difference in their behavior is in the manner of application of load, i.e. in one case referred to as BH, the load is applied at the ends of the plate, and in the other case (BB), the load is introduced through bolt bearing on the hole surface, which resembles a more realistic situation. The third has a dog-bone shape which is meant to mimic the flange of a beam with the post-Northridge reduced beam section (RBS) type detail.

The BH – Bolt Hole Specimens

A schematic of a BH specimen is shown in Fig. 7. These specimens are machined from a 2" X 1" X 6" plate, and the central 3 inches of the plate are reduced in thickness to 0.375 inch, whereas the ends of the plates have holes through which pins attach the specimen to the load frame. The load is applied to the specimen at the ends by means of pins which are connected to the actuator by means of an elaborate fixture. The smaller thickness of the plate forces failure to occur at the section through the bolt holes. The average specimen elongation is measured using LVDTs (Linear Voltage Displacement Transducers) mounted on either side of the specimen to account for rocking of the specimen.

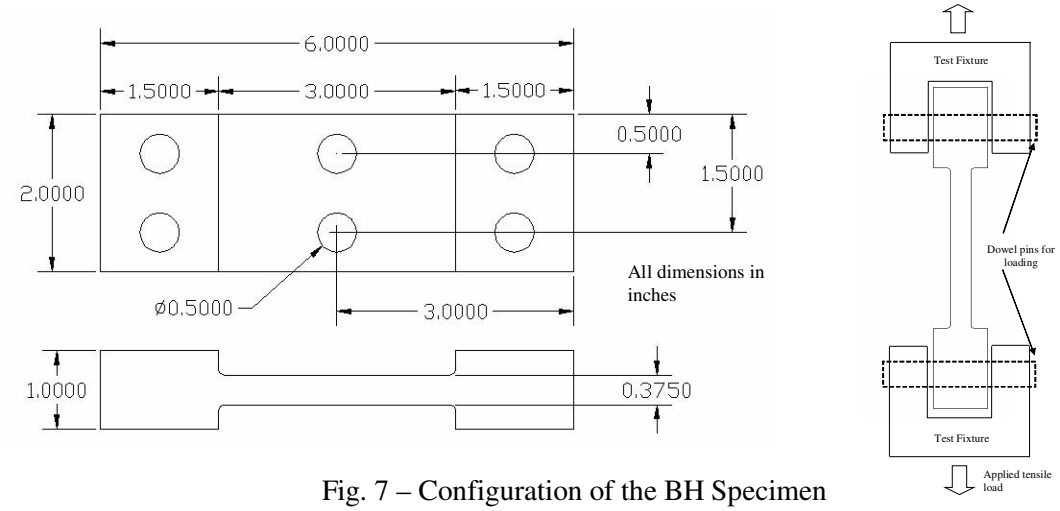

Fig. 7 – Configuration of the BH Specimen

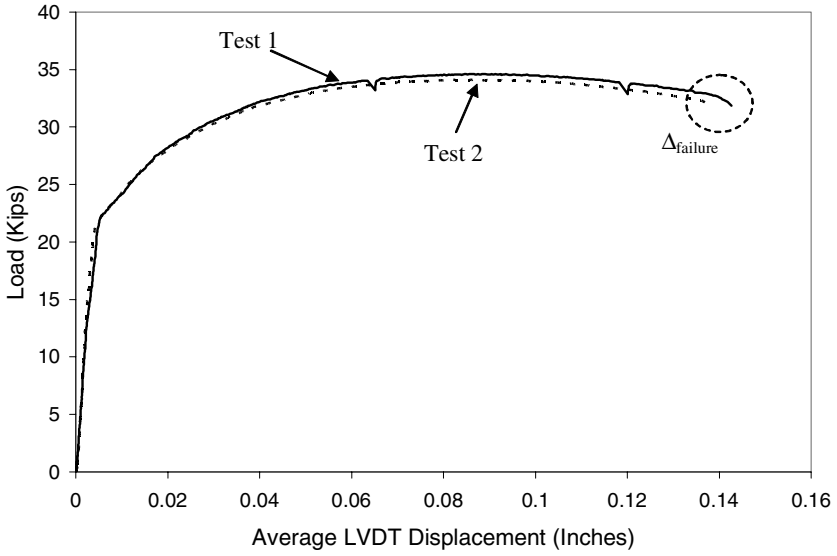

Fig. 8 – Load Displacement Curve for BH Test, A572 Grade 50 Steel

Fig. 8 shows a representative load displacement curve for such a test (shown here for the A572 Grade 50 Steel). As the test begins, the load rises to reach a maximum, at which point the steel ligaments between the holes start to neck, and the load starts dropping. After this point, the plastic strain increases until a critical value of plastic strain is encountered, and the material fractures. The fracture typically initiates at the bolt hole in the outside ligament. Rupture of the outside ligament causes a significant load drop, and further straining causes the middle ligament to fail as well. For purposes of this study, the first failure, i.e., the failure of the edge ligament is considered to be the point of fracture and the corresponding displacement $\Delta_{failure}$ is considered to be the failure displacement. A total of four such tests is conducted (two for each of the steel varieties). Both materials show failure displacements in the range of 0.15 to 0.20 inches. Finite element analyses are presented in a subsequent section.

The BB – Bolt Bearing Specimens

In bolted connections, load is introduced to the base metal by the bolts bearing on the inner surface of the holes. This is distinct from the BH specimen where the load is introduced at the end of the specimen. Design formulae and equations make no distinction between the two situations. However, it is of interest to investigate if indeed the two exhibit the same behavior and differences are observed in the FEM analyses.

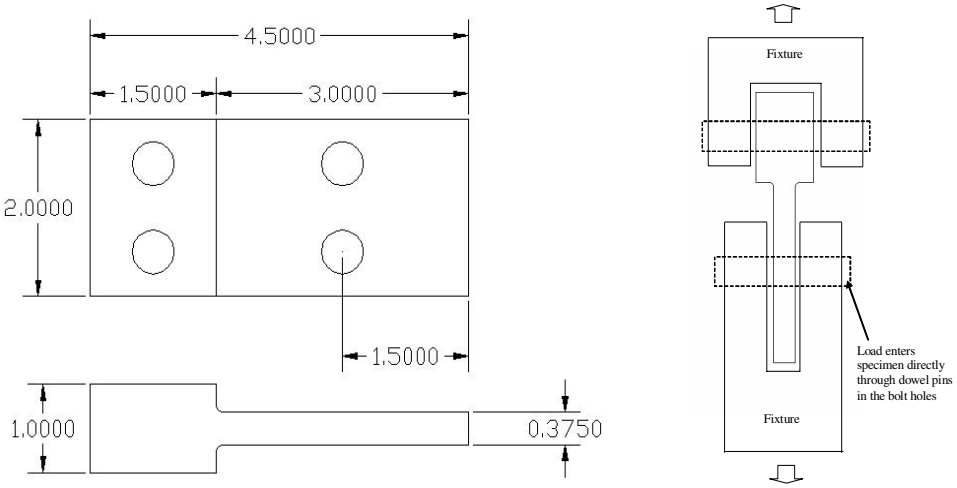

Fig. 9 – Configuration of the BB Specimen

To compare with the tests with the BH tests, we run companion tests that are more realistic, i.e. instead of pulling on the ends of the plate and causing failure in the middle at the location of the boltholes, the load is applied by means of pins passing through the bolt holes as shown in Fig. 9.

The BB specimens exhibited behavior nearly identical to the BH specimens, with fracture initiation in the ligament at the edge of the specimen and similar load-deflection curves. The load displacement curves look very similar (in nature and in magnitude) to that in BH. For all the specimens, elongation to failure is in the range 0.15-0.20 inches which is comparable with the elongation seen for the BH tests.

The Reduced Beam Section (RBS) Specimen

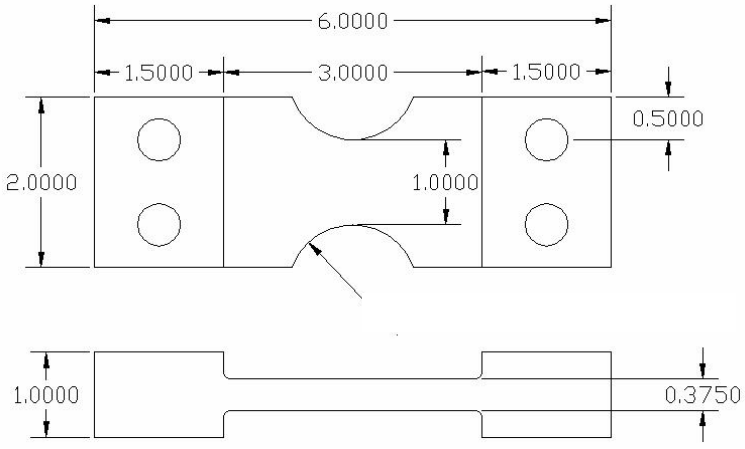

Fig. 10 – Configuration of the RBS specimen

Reduced Beam Section (RBS), or dog-bone connections aim to reduce the total stress and strain demand on the welded joint, lowering the fracture tendency. However, the steel is still prone to ductile crack initiation in the highly strained dog-bone region. Four RBS pull-plate tests (two for each steel variety), were conducted to investigate the abilities of the SMCS model in characterizing such failures. The basic geometry of the specimen is shown in Fig. 10. The overall geometry of the specimen is similar to that of the BH specimen, except that the central part of the plate is narrowed down to a width of 1 inch.

The load displacement curves are similar in nature to the BH and BB specimens. The fracture seems to occur in an instant suggesting that the ductile initiation takes place simultaneously over a large area until of a sudden the material fails by a mixture of tearing and ductile mechanisms. The fracture elongations are in the range of 0.20-0.25 for both the steel types.

MICROMECHANICAL SIMULATION OF DUCTILE CRACK INITIATION IN THE PULL-PLATE TYPE EXPERIMENTS

Three dimensional finite element models are constructed for all the geometries, i.e. the BH, BB and the RBS to capture complicated behavior such as out of plane necking. The models are built in ABAQUS/CAE 6.2 and use large deformation theory and isotropic incremental plasticity. The finite element models for all the three configurations are similar, and moreover the fracture prediction methodologies based on the SMCS model are identical. For illustration purposes, we briefly summarize the fracture prediction process for the BB configuration, recognizing that a similar process for adopted for the other configurations as well.

The BB configuration has two planes of symmetry, so it is sufficient to construct a quarter-sized FEM model. Fig. 11 shows the deformed model with the equivalent plastic strain contours. The boundary conditions are fixed according to the requirements of symmetry, and the model is loaded in displacement control. The finite element mesh has just under 1000 hexahedral elements, and the size of smallest elements (in the regions of fracture is of the order of 0.03 inches).

This is a seemingly economical mesh, considering that the aim of the model is to simulate the micromechanical process of void growth and coalescence that typically take place at much smaller length scales. However, the extremely flat stress-strain gradients in the geometries under consideration allow us to coarsen the mesh to this extent. The analysis requires approximately 20 minutes to run on a Pentium 4, 1.4 GHz processor.

To examine failure in the test specimens, we monitor the stress and strain contours over the entire region of the critical section of the specimen. The SMCS criteria is found to be the triggered first at the location indicated in Fig. 11 and the stress strain profiles are sufficiently flat in the nearby vicinity such that for a very small increment in global displacement, the SMCS is suddenly satisfied over a very large area. The global displacement corresponding to the instant in the loading history where the SMCS reaches a value of zero is calculated as the analytical prediction of the failure displacement corresponding to ductile crack initiation – $\Delta_{failure}^{Analysis}$. Fig. 12 shows the analysis plot and failure prediction overlaid on the experimental observations (for the A572 steel) where there is good agreement between both the predicted fracture displacement and the overall load-deflection response.

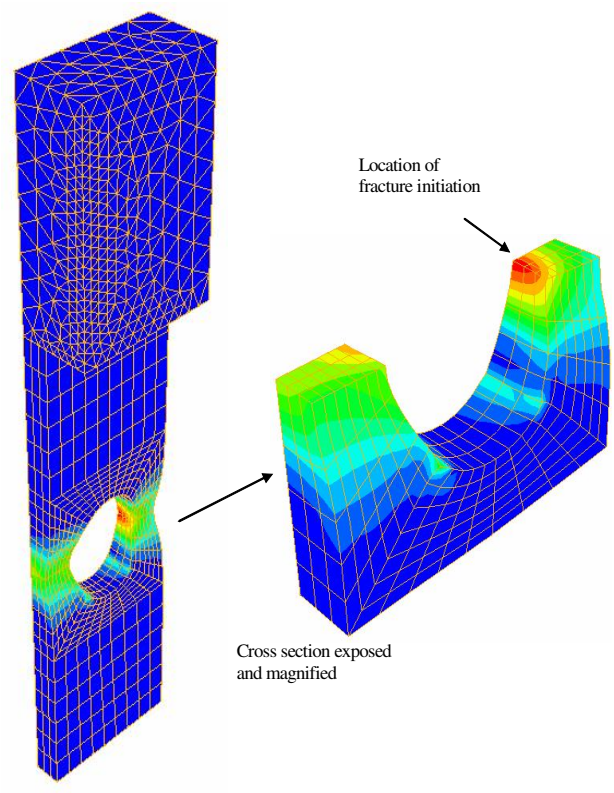

Fig. 11 – Deformed FEM mesh of BB specimen showing plastic strain contours and location of ductile crack initiation

A similar procedure is carried out for the BH and the RBS specimens, where predictions of ductile crack initiation are compared with the experimentally observed point of failure. Table 2 (a), (b) and (c) summarize the experimental results and the analytical predictions (based on the SMCS model) of ductile crack initiation for the BH, BB and the RBS configurations.

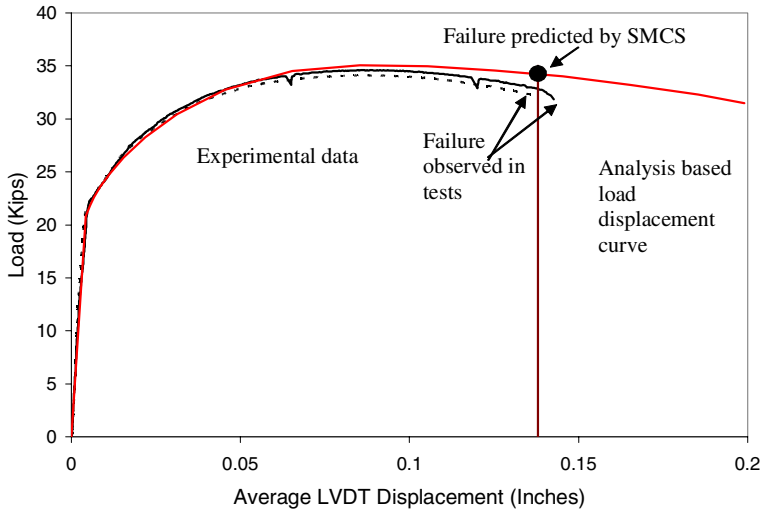

Fig. 12 – Failure Prediction in BB Specimens using SMCS

Table 2(a) – BH Tests and Analyses

Steel	Test	$\Delta_{failure}^{Test}$ (inches)	$\Delta_{failure}^{Analysis}$ SMCS (inches)
A572	BH1	0.14	0.14
A572	BH2	0.14	
HPS70W	BH1	0.14	0.18
HPS70W	BH2	0.15	

Table 2(b) – BB Tests and Analyses

Steel	Test	$\Delta_{failure}^{Test}$ (inches)	$\Delta_{failure}^{Analysis}$ SMCS (inches)
A572	BB1	0.15	0.14
A572	BB2	0.14	
HPS70W	BB1	0.16	0.18
HPS70W	BB2	0.16	

Table 2(c) – RBS Tests and Analyses

Steel	Test	$\Delta_{failure}^{Test}$ (inches)	$\Delta_{failure}^{Analysis}$ SMCS (inches)
AP50	RBS1	0.25	0.26
AP50	RBS2	0.25	
AP70HP	RBS1	0.22	0.24
AP70HP	RBS2	0.21	

In all the cases, the model predicted the location of ductile fracture accurately, and the ductility within a 10-15% error limit. In most situations, the difference between the predicted failure elongation and the experimentally observed failure deformation is within a 10% error range. This indicates that the SMCS model is an efficient tool for predicting ductile crack initiation in civil engineering steels in structure like configurations.

A general trend that can be observed from all the tests is that while the measured values of the failure displacement are fairly consistent for each configuration, there is a consistent bias in the predicted values, in the sense that the values predicted for the HPS70W are slightly higher than those for the A572. There are two possible explanations for this bias. The first is that the SMCS model is based on the instantaneous values of stress and strain fields, whereas the void growth and coalescence process involves the integration of stress and strain histories, see Rice et al [5]. This evolution is not captured by the SMCS model, which is based on the assumption of the independence of triaxiality and plastic strain – an assumption that is valid under small displacements and geometry changes. The HPS70W steel is more ductile as compared to the A572 steel, and as a result, the geometry changes are larger, likely invalidating the assumptions of the SMCS model. Another model, the Void Growth Model (VGM), refer Rice [5], makes better predictions of failure in some cases – Kanvinde [3]. Another reason for the discrepancy could be linked to the fact that the HPS70W has a higher ultimate stress (100 ksi) as compared to the A572 (85 ksi). As a result, some of the HPS70W specimens showed regions of cleavage fracture interspersed with ductile tearing – raising doubts about what process initiated the failure – cleavage or void growth. In case it is cleavage, then the SMCS would not be able to capture the mechanism of failure.

Looking at the load-displacement graphs, there is no apparent difference between the test data for the BH and the BB tests. FEM analyses and data are useful to investigate whether there is a similarity in the evolution of the stress and strain fields that actually drive the fracture process under the two situations to compare and contrast the similarities and differences. Fig. 13 shows the plot of the SMCS at the critical location versus the specimen elongation for the BB and the BH geometries. It is interesting to note that for both the steels, the graphs of SMCS versus specimen elongation are virtually coincident, thus confirming that the stress-strain fields and resulting fracture behavior is also quite similar.

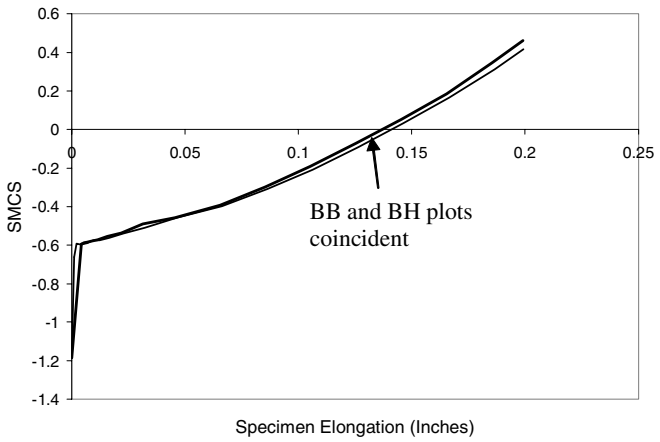

Fig. 13 – Comparison between BB and BH response

DISCUSSION AND CONCLUSIONS

A number of interesting conclusions can be drawn from experimental and analytical components of this study. The key issues can be summarized as follows:

1. The Stress Modified Critical Strain (SMCS) model can predict ductile crack initiation with good accuracy under situations of large-scale yielding in flaw-free geometries. The predictions are accurate both in terms of the location of fracture, as well as the ductility or strain at fracture.

2. For structural components without flaws, the SMCS model is especially convenient to use, because the shallow stress-stress contours allow for a coarse mesh. As a result, the micromechanical simulations can be performed with relatively minimal computational expense.
3. The SMCS model can be used to make important behavioral inferences regarding fracture, which can enhance fundamental understanding of behavior, and aid the transfer of test results from one situation to another.
4. The structural situations considered here do not have sharp cracks and flaws, and as such are not sensitive to the length scale issues. The application of the SMCS criterion to situations with sharper stress-strain gradients has not been verified in this paper.
5. Structures undergo cyclic loading or low-cycle fatigue in earthquakes. This paper primarily deals only with monotonic loading. The transferability of the SMCS results to such situations is an issue not addressed in this paper. For this, we refer the reader to a larger study by the authors – Kanvinde [3], which develops and demonstrates micromechanical models for low cycle fatigue. The larger study was comprehensive in the sense that it included seven steel varieties (four obtained in the USA and three obtained from Nippon Steel Corporation, Japan). The steels included high-strength plate steels, as well as special bridge steels. The larger study included over two-hundred tests, and complementary finite element analyses. It demonstrated the use of micromechanical models for prediction of structural fracture in metals and structures. It also developed new models for ultra-low cycle fatigue of steel connections during cyclic earthquake loading.

To summarize, the SMCS model is found to be a valuable and surprisingly convenient tool to predict ductile crack initiation in some structural engineering components. Micromechanical models similar to the SMCS can help in more realistic simulation of structures, with relatively few assumptions, and can be extended to a variety of situations such as low-cycle fatigue or brittle cleavage fracture. The authors are grateful to the National Science Foundation and the Nippon Steel Corporation, for financial and technical assistance on this project.

REFERENCES

1. Chi W-M, Deierlein, G.G., Ingraffea, A.R. “Finite Element Fracture Mechanics Investigation of Welded Beam-Column Connections,” SAC/BD-97/05, National Information Service for Earthquake Engineering, Berkeley, CA. 1976
2. Hancock, J. W. and Mackenzie, A. C. “On the mechanics of ductile failure in high-strength steel subjected to multi-axial stress-states,” Journal of Mechanics and Physics of Solids, Vol. 24, 1976, pp. 147-169, 1976.
3. Kanvinde, A.M. “Micromechanical Simulation of Earthquake Induced Fractures in Steel Structures.” Ph.D. Thesis submitted to Stanford University. 2004.
4. Panontin, T. L. and Sheppard, S. D. “The relationship between constraint and ductile fracture initiation as defined by micromechanical analyses,” Fracture Mechanics: 26th Volume. ASTM STP 1256, 1995
5. Rice, J. R. “On the ductile enlargement of voids in triaxial stress fields,” Journal of the Mechanics and Physics of Solids, Vol. 17, 1969, pp. 201-217, 1969.
6. Stojadinovic, B., Goel, S., and Lee, K.H., “Development of post-Northridge steel moment connections.” Proceedings of the12th World Conference on Earthquake Engineering, New Zealand, paper 1269, 2000.